Mechanism of phase transitions and electronic density of states in $LaFeAsO_{1-x}F_x$ and $SmFeAsO_{1-x}F_x$ from *ab initio* density functional calculations

Peter V. Sushko,[1,2,*] Alexander L. Shluger,[1,2] Masahiro Hirano,[3] and Hideo Hosono[3,*]

[1]*WPI Advanced Institute for Materials Research, Tohoku University, 2-1-1 Katahira, Aoba, Sendai 980-8577, Japan*

[2]*Department of Physics and Astronomy, London Centre for Nanotechnology, Materials Simulation Laboratory, University College London, Gower Street, London WC1E 6BT, United Kingdom*

[3]*Frontier Collaborative Research Center and Materials and Structures Laboratory, Tokyo Institute of Technology, 4259 Nagasuta, Midori-ku, Yokohama 226-8503, Japan*

(Received 20 October 2008; published 25 November 2008)

The structure and electronic density of states in layered $LFeAsO_{1-x}F_x$ (L=La,Sm; x=0.0,0125,0.25) are investigated using density functional theory. For the x=0.0 system we predict a complex potential-energy surface, formed by close-lying single-well and double-well potentials, which give rise to the tetragonal-to-orthorhombic structural transition and the appearance of magnetic order. For $x>0.0$ we demonstrate that transition temperatures to the superconducting state and their dependence on x correlate well with the calculated magnitude of the electronic density of states at the Fermi energy.

DOI: 10.1103/PhysRevB.78.172508 PACS number(s): 74.25.Jb, 61.50.Ah, 75.25.+z

The discovery of a new superconductor $LaFeAsO_{1-x}F_x$ with high transition temperature (T_c=26 K) (Ref. 1) has triggered a global search for other Fe-based alternatives to Cu-based superconductors, which have dominated the field since 1986.[2] Substituting As, Fe, and La for other pnicogens,[3] transition metals,[4] and lanthanides,[5] respectively, as well as applying external pressure[6] and optimizing the doping level have raised T_c to 54.5 K.[7] However, since then its value seems to have saturated, and doubts have been expressed as to whether T_c can be raised any further.[8] Electronic structure calculations can provide insight into the properties of these systems and their relation to T_c.

LaFeAsO is a member of the layered Fe-pnicogens, in which FeAs sheets are separated from each other by spacers such as layers of metal oxide, e.g., LaO in LaFeAsO [Fig. 1(a)], metal fluoride, e.g., SrF in SrFeAsF,[9] and metal atoms, e.g., Ba in $BaFe_2As_2$.[10] In spite of the difference in the nature of the spacers, FeAs-based materials show surprising similarities in the temperature dependence of their structural parameters and anomalies in electric resistance and specific-heat capacity and in their magnetic properties (e.g., Refs. 10–14). Transition to a superconducting state has been observed in Fe-pnictides doped in both the spacer layers (e.g., Refs. 15 and 16) and Fe layers.[9]

In a series of theoretical and computational reports the electronic properties, magnetic interactions, phonon structure, and the origin of the superconductivity in LaFeAsO and related compounds have been discussed (e.g., Refs. 17–24). The aim of this work is twofold: (i) to investigate the relation between the magnetic and atomic structures of FeAs-based materials and (ii) to study the effect of the electron doping on the electronic properties of these systems.

We found that the properties of LFeAsO (where L =La,Sm) are determined by two close-lying potential-energy surfaces (PESs): a lower-energy double-well potential, where geometrical configurations of the two energy minima have orthorhombic (**O**) symmetry, and a higher-energy single-well potential of tetragonal (**T**) lattice symmetry. This complex PES gives rise to three temperature ranges—and, therefore, two transition temperatures—and can explain the experimentally observed structural phase transition, the appearance of magnetic order, and the anomaly in the temperature dependence of the specific-heat capacity. In addition, we noticed a correlation between the calculated profile of the electronic density of states $[N(\varepsilon)]$ near the Fermi energy (ε_F) and the experimentally observed dependence of T_c on the dopant concentration x and on the type of L atom. This correlation can be used for computational prescreening of promising LFeAsO derivatives, as well as for predicting optimal dopant concentrations via relatively inexpensive electronic structure calculations.

The calculations were carried out using density functional theory (DFT), the generalized gradient approximation functional PW91,[25] and the projected augmented waves method[26] implemented in the Vienna *ab initio* simulation program (VASP) code.[27] The plane-wave basis set cutoff was set to 600 eV. Supercells containing eight (1×1), 16 ($\sqrt{2}\times\sqrt{2}$), and 32 (2×2) atoms and Monkhorst-Pack grids of 252, 132, and 36 k points, respectively, were used. For the analysis of the electronic structure, the charge density was decomposed over atom-centered spherical harmonics.

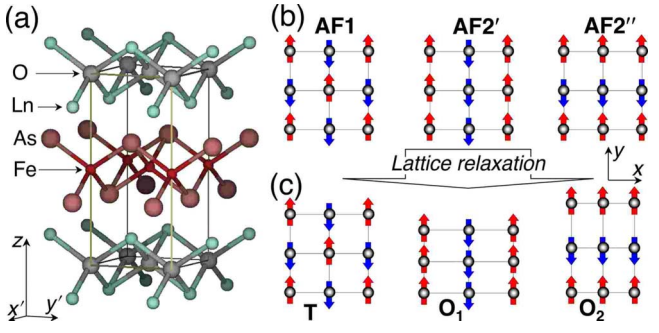

FIG. 1. (Color online) (a) Structure of the 1×1 LFeAsO (L =La,Sm) unit cell. (b) Schematics of several spin configurations within the Fe layers shown for a $\sqrt{2}\times\sqrt{2}$ supercell. The circles show the positions of Fe atoms within the Fe layer. Here and below, up and down arrows indicate "up" and "down" spins, respectively. See text for details.

TABLE I. Structural parameters of LFeAsO$_{1-x}$F$_x$ (L=La,Sm). Parameters a and b are given for the $\sqrt{2}\times\sqrt{2}$ cell. In all cases, crystallographic cell angles α, β, and γ deviate from 90° by less than 0.0005°. Letters E and T refer to experiment and theory (this work), respectively. There are two types of L and As atoms for x =0.125.

x	Details		a (Å)	b (Å)	c (Å)	$z(L)$	z(As)
			LaFeAsO$_{1-x}$F$_x$				
0.0	AF1	T	5.6873	5.6899	8.6185	0.1448	0.6383
0.0	AF2	T	5.7305	5.6672	8.6948	0.1433	0.6438
0.0	300 K	E [a]	5.7031	5.7031	8.74111	0.1413	0.6517
0.0	120 K	E [a]	5.6826	5.7104	8.71964	0.1417	0.6513
0.125		T	5.6829	5.6829	8.5630	0.1560	0.6405
						0.1452	0.6394
0.25		T	5.6873	5.6831	8.4859	0.1562	0.6410
0.14	120 K	E [a]	5.6844	5.6844	8.6653	0.1477	0.6527
			SmFeAsO$_{1-x}$F$_x$				
0.0	AF1	T	5.5955	5.5918	8.3435	0.1406	0.6472
0.0	AF2	T	5.5834	5.5834	8.2884	0.1523	0.6496
0.125		T	5.5834	5.5834	8.2884	0.1523	0.6496
						0.1413	0.6479
0.25		T	5.5888	5.5902	8.2046	0.1529	0.6493

[a]Reference 11.

First, we consider the relation between configurations of the spins associated with Fe 3d electrons and the lattice structure. Several ordered antiferromagnetic configurations in the $\sqrt{2}\times\sqrt{2}$ supercell are shown in Fig. 1(b). In AF1, the spins on the neighboring Fe atoms are antiparallel. In configurations AF2′ and AF2″ spins are parallel along the y and x axes, respectively; AF2′ and AF2″ are equivalent in the case of the tetragonal phase [Fig. 1(b)].

After minimization of the total energy with respect to both the atomic positions and the lattice parameters, the AF1 configuration maintains the **T** structure (Table I). Configurations AF2′ and AF2″ relax to two equivalent orthorhombic (**O**) structures $\mathbf{O}_1$ and $\mathbf{O}_2$, in which the Fe 3d spins along the short Fe-Fe bonds are parallel and those along the long Fe-Fe bonds are antiparallel [see Fig. 1(c)]. The relations between lattice parameters a, b, and c for $\mathbf{O}_1$ and $\mathbf{O}_2$ are $a_1=b_2$, $b_1=a_2$, $c_1=c_2$, and $a_1>b_1$ (see also Fig. 2). The calculated values for the lattice parameters for the low-temperature **O** phase agree with experimental data to within 0.4%. (Table I). The ferromagnetic configuration is considerably less stable than the antiferromagnetic ones and is not considered here.

Integration of the AF2″ charge density within the LaO and FeAs layers shows that the layers are charged: $(\mathrm{LaO})^{+\delta}(\mathrm{FeAs})^{-\delta}$ with $\delta=0.15|e|$. Thus, one can consider LFeAsO as a superionic compound in which ionic and ion-covalent bondings within the LO and FeAs layers, respectively, are accompanied by ionic bonding of these layers. The magnetic moments on the Fe atoms calculated for AF2 are $1.56\mu_B$ (L=La) and $1.33\mu_B$ (L=Sm). These differ significantly from the values suggested by Mössbauer measurements ($\sim 0.35\mu_B$).[28] The calculated aspect ratio $\Delta=(a/b-1)$ is overestimated: we find that $\Delta=1.1\%$ for both oxides, while the experimental values are 0.5% for L=La (Ref. 11) and 0.7% for L=Sm.[14]

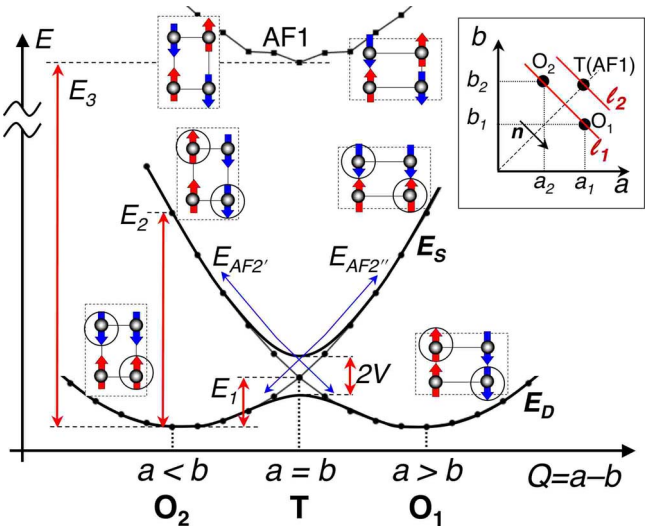

FIG. 2. (Color online) Potential-energy surfaces for the AF1 and AF2 configurations. Dots correspond to the calculated energy values. Circles indicate spin pairs within the Fe layer in the $\sqrt{2}\times\sqrt{2}$ cell, which are different in $\mathbf{O}_1$ and $\mathbf{O}_2$ configurations.

To find the energy barrier separating the fully relaxed AF2′ and AF2″ configurations, we calculated the total energies $E_{\mathrm{AF2}'}$ and $E_{\mathrm{AF2}''}$ along the path ℓ_1 connecting $\mathbf{O}_1$ and $\mathbf{O}_2$ (inset in Fig. 2). Path ℓ_1 is parallel to the vector $\mathbf{n}=(1,-1)$ in the a-b plane. $E_{\mathrm{AF2}'}(Q)$ and $E_{\mathrm{AF2}''}(Q)$, where $Q=a-b$, are plotted in Fig. 2. For comparison, we also calculated $E_{\mathrm{AF1}}(Q)$ along the path $\ell_2\|\mathbf{n}$.

The calculated values of E_1, E_2, and E_3 (Fig. 2) are 0.005, 0.025, and 0.15 eV, respectively, for LaFeAsO and 0.006, 0.026, and 0.11 eV for SmFeAsO.[29] The terms $E_{\mathrm{AF2}'}$ and $E_{\mathrm{AF2}''}$, calculated within the adiabatic DFT approximation, are degenerate at $Q=0$. In practice, tunneling between their respective electronic states will couple these states and split $E_{\mathrm{AF2}'}$ and $E_{\mathrm{AF2}''}$ terms by 2 V into a higher-energy single-well (E_S) and a lower-energy double-well (E_D) PESs,[30] as shown in Fig. 2.

The lattice dynamics, described by E_S and E_D, has three regimes depending on the temperature (T).

(1) For $T<E_1-V$, the atoms vibrate near the positions defined by one of the orthorhombic energy minima of E_D (e.g., $\mathbf{O}_1$). In this case the magnetic structure is dominated by AF2′ configuration (see Fig. 2).

(2) For $E_1-V<T<E_1+V$, atomic motion is determined by both minima of E_D. In the classical picture of the atom dynamics, the time-average distribution of the Fe-Fe bond lengths has two maxima. As T increases, the splitting between the short and the long Fe-Fe bonds decreases, which corresponds to a gradual transition from **O** to **T** symmetry. Magnetic order is lost because the Fe spins adjust themselves to the momentary local atomic structure so that the spins are parallel for Fe atoms forming short Fe-Fe bonds, and antiparallel otherwise. In other words, thermal fluctuations of Fe-Fe bond lengths cause the reorientation of Fe spins (Fig. 2).

(3) For $T > E_1 + V$, the lattice dynamics is determined by both the E_S and E_D potentials and the effect of the barrier in E_D can be neglected. The lattice has **T** symmetry. There is no magnetic order because the orientation of the spins changes according to the local atomic structure, as described in regime (2), and also due to the coupling of the electronic states of E_S and E_D.

This model accounts for the main effects observed experimentally in LaFeAsO and related materials. For example, observations of the structural and magnetic phase transitions in LaFeAsO (e.g., Refs. 11, 13, and 31) suggest that the $\mathbf{T} \rightarrow \mathbf{O}$ transition takes place gradually, with the $Q = a - b$ order parameter exhibiting two kinks at $T_{\max}$ (~160 K) and $T_{\min}$ (~140 K), and that the magnetic phase transition occurs at $T_{\min}$ or slightly below it. In addition, the specific-heat capacity displays two peaks, which also seem to coincide with $T_{\max}$ and $T_{\min}$.[12,13] Similar data have been reported for other FeAs-based materials.[10] These results are consistent with the model for the three regimes of the lattice dynamics outlined above. In this model, two phase transition temperatures $T_{\max}$ and $T_{\min}$ would correspond to $E_1 + V$ and $E_1 - V$, respectively. While calculating the value of V is beyond the scope of this work, we can use the experimental results[13,12] to estimate that $V \approx 4$ cm^{-1} in LaFeAsO.

We note that similar magnetoelastic effects, i.e., a magnetic phase transition associated with a structural **T**-**O** transition, have been observed in pnictides, oxides, and complex compounds of rare-earth elements.[32–34] In this case, the temperature of the structural phase transition is lower (~4–30 K) due to more localized f states. Consistent with this, the difference between $T_{\max}$ and $T_{\min}$ becomes vanishingly small. For example, it is below the resolution limit in $ErNi_2B_2C$,[34] while for $DyVO_4$ the value of V is estimated to be 1.5 cm^{-1}.[33]

We now consider the effect of F doping on the atomic and electronic structures of LFeAsO. This doping provides additional electrons to the FeAs layer so that the charge distribution becomes $(LO)^{+\delta+x}(\mathrm{FeAs})^{-\delta-x}$, and the lattice parameter c decreases due to the increased interlayer ionic bonding (Table I). This leads to the appearance of a narrow gap in $N(\varepsilon)$ at ~2.5 eV below the ε_F (not shown).

The lowest energy state in the 2×2 cell ($x = 0.125$) is similar to that of undoped LFeAsO: the lattice structure corresponds to the **O** symmetry of the $\sqrt{2} \times \sqrt{2}$ cell and the spin-arrangement is the same as that in AF2. However, the value of the aspect ratio Δ decreases to 0.8% and 0.7% for the L=La and L=Sm, respectively. Simultaneously, the value of μ_{Fe} is reduced to 1.32 (L=La) and $0.75\mu_B$ (L=Sm). At higher doping levels ($\sqrt{2} \times \sqrt{2}$ cell, $x = 0.25$) $\Delta < 0.07\%$. In addition, μ_{Fe} reduces further to below $0.1\mu_B$ and the AF2 magnetic order vanishes: the spin-down density is localized on a single Fe atom nearest to the F^- impurity, while the remaining three Fe atoms share the spin-up density. We also found a spin-disordered state for $x = 0.125$: this corresponds to a nearly tetragonal cell (Table I) with an energy of ~7 meV (L=La) and ~5 meV (L=Sm) per Fe atom higher than that of the ground state. Thus, with increasing x the extent of the orthorhombic distortion decreases and the magnetic structure is modified.

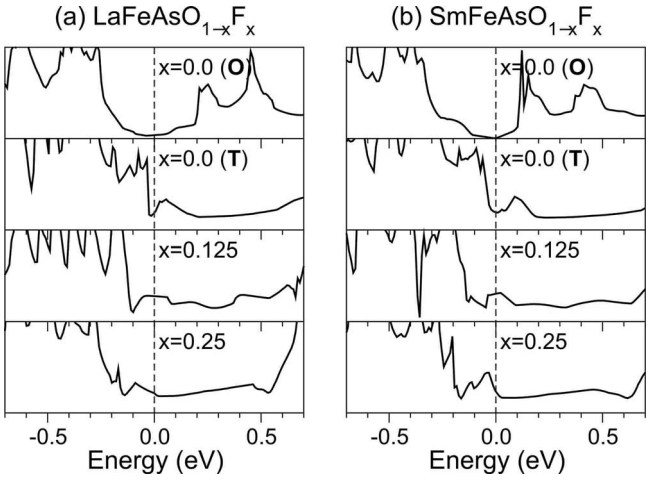

FIG. 3. Density of states for $(\mathrm{La,Sm})\mathrm{FeAsO}_{1-x}\mathrm{F}_x$. Letters **O** and **T** refer to the orthorhombic and tetragonal phases, respectively. The Fermi energy is at 0.0 eV.

Finally, we analyze the electronic density of states $[N(\varepsilon)]$ calculated for the fully relaxed AF1, AF2, and spin-disordered states of doped $L\mathrm{FeAsO}_{1-x}\mathrm{F}_x$ (Fig. 3). In all cases, $N(\varepsilon)$ near the Fermi energy (ε_F) is dominated by the Fe $3d$ states, and the overall polarization of the spin-up and spin-down states is negligible. In stoichiometric LFeAsO, $N_{\mathrm{AF2}}(\varepsilon)$ has a pronounced depression near ε_F, while $N_{\mathrm{AF1}}(\varepsilon)$ has a narrow deep minimum separating a steep rise at $\varepsilon < \varepsilon_F$ and a peak at $\varepsilon > \varepsilon_F$.[35] Projecting $N_{\mathrm{AF1}}(\varepsilon)$ onto the d states shows that this peak is dominated by d_{xz} and d_{yz} states. The same $d_{xz} + d_{yz}$ peaks near ε_F are evident for doped LFeAsO (Fig. 3).

We notice that as x increases and ε_F shifts across the $d_{xz} + d_{yz}$ peak, the value of $N(\varepsilon_F)$ increases as well, reaches its maximum, and then decreases. The details of the peak structure depend on the value of x, but its general shape is reminiscent of the experimentally observed dependence of T_c on x (e.g.[1,14]).

Furthermore, the maximum of the $d_{xz} + d_{yz}$ peak ($x = 0.0$) in SmFeAsO is higher and further away from ε_F than that in LaFeAsO. This correlates with the observations that the optimal T_c is higher in $\mathrm{SmFeAsO}_{1-x}\mathrm{F}_x$ [46 K, $x = 0.15$ (Ref. 5)] than in $\mathrm{LaFeAsO}_{1-x}\mathrm{F}_x$ [26 K, $x = 0.05$–0.12 (Ref. 1)] and that it is achieved at larger values of x. The slope of $N(\varepsilon_F)$ calculated for $x = 0.125$ is negative for L=La and positive for L=Sm, which indicates that the maximum of $N(\varepsilon_F)$ can be found at $x < 0.125$ for L=La and $x > 0.125$ for L=Sm. This is consistent with the optimal values of x found for these compounds as ~0.11 (L=La) (Ref. 1) and ~0.20 (L=Sm).[14] In addition, we notice that the $d_{xz} + d_{yz}$ peak in LaFeAsO is wider than that in SmFeAsO (this is clearly seen for $x = 0.0$ and 0.125), which suggests that T_c has a stronger dependence on x in SmFeAsO, as observed in Ref. 14.

While these observations say little about the mechanism of superconductivity in FeAs-based materials, they do not contradict recent experimental results indicating that these materials have common features with conventional Bardeen-Cooper-Schrieffer-type superconductors.[36] More importantly, our analysis suggests that the value of $N(\varepsilon_F)$ is a good

parameter for T_c optimization.[37] Our results indicate that the chemical nature of the spacers between FeAs layers does not directly affect the superconducting state. We suggest that its properties are mainly determined by the coupling of Fe spins with phonons modulating Fe-Fe distances.

The authors are grateful to C. Rüegg, A. M. Stoneham, Z. Tesanovic, Z.-Y. Lu, and M. Wolf for their comments on the manuscript, and S. W. Kim, Y. Kamihara, T. Nomura, T. Kamyia, G. Kresse, and E. K. U. Gross for valuable discussions. P.V.S. is supported by the Grant-in-Aid for Creative Scientific Research (Grant No. 16GS0205) from the Japanese Ministry of Education, Culture, Sports, Science and Technology, WPI-AIMR at Tohoku University, and the Royal Society. The access to HPCx is provided via the Materials Chemistry Consortium.

*p.sushko@ucl.ac.uk

[1] Y. Kamihara, T. Watanabe, M. Hirano, and H. Hosono, J. Am. Chem. Soc. **130**, 3296 (2008).
[2] J. G. Bednorz and K. A. Muller, Z. Phys. B: Condens. Matter **64**, 189 (1986).
[3] Y. Kamihara, H. Hiramatsu, M. Hirano, R. Kawamura, H. Yanagi, T. Kamiya, and H. Hosono, J. Am. Chem. Soc. **128**, 10012 (2006).
[4] T. Watanabe, H. Yanagi, T. Kamiya, Y. Kamihara, H. Hiramatsu, M. Hirano, and H. Hosono, Inorg. Chem. **46**, 7719 (2007).
[5] X. H. Chen, T. Wu, G. Wu, R. H. Liu, H. Chen, and D. F. Fang, Nature (London) **453**, 761 (2008).
[6] H. Takahashi, K. Igawa, K. Arii, Y. Kamihara, M. Hirano, and H. Hosono, Nature (London) **453**, 376 (2008).
[7] J. Yang, Z.-C. Li, W. Lu, W. Yi, X.-L. Shen, Z.-A. Ren, G.-C. Che, X.-L. Dong, L.-L. Sun, F. Zhou, and Z.-X. Zhao, Supercond. Sci. Technol. **21**, 082001 (2008).
[8] P. M. Grant, Nature (London) **453**, 1000 (2008).
[9] S. Matsuishi, Y. Inoue, T. Nomura, M. Hirano, and H. Hosono, arXiv:0810.2351, J. Phys. Soc. Jpn. (to be published).
[10] M. Rotter, M. Tegel, D. Johrendt, I. Schellenberg, W. Hermes, and R. Pottgen, Phys. Rev. B **78**, 020503(R) (2008).
[11] T. Nomura *et al.*, J. Phys. Soc. Jpn. (unpublished).
[12] Y. Kohama, Y. Kamihara, M. Hirano, H. Kawaji, T. Atake, and H. Hosono, Phys. Rev. B **78**, 020512(R) (2008).
[13] M. A. McGuire, A. D. Christianson, A. S. Sefat, B. C. Sales, M. D. Lumsden, R. Jin, E. A. Payzant, D. Mandrus, Y. Luan, V. Keppens, V. Varadarajan, J. W. Brill, R. P. Hermann, M. T. Sougrati, F. Grandjean, and G. J. Long, Phys. Rev. B **78**, 094517 (2008).
[14] S. Margadonna, Y. Takabayashi, M. Mcdonald, M. Brunelli, G. Wu, R. Liu, X. Chen, and K. Prassides, arXiv:0806.3962 (unpublished).
[15] X. Zhu, F. Han, P. Cheng, G. Mu, B. Shen, and H. Wen, arXiv:0810.2531 (unpublished).
[16] X. Zhu, F. Han, P. Cheng, G. Mu, B. Shen, and H.-H. Wen, Europhys. Lett. **82**, 17009 (2008).
[17] K. Haule, J. H. Shim, and G. Kotliar, Phys. Rev. Lett. **100**, 226402 (2008).
[18] D. J. Singh and M.-H. Du, Phys. Rev. Lett. **100**, 237003 (2008).
[19] S. Ishibashi, K. Terakura, and H. Hosono, J. Phys. Soc. Jpn. **77**, 053709 (2008).
[20] I. I. Mazin, D. J. Singh, M. D. Johannes, and M. H. Du, Phys. Rev. Lett. **101**, 057003 (2008).
[21] K. Kuroki, S. Onari, R. Arita, H. Usui, Y. Tanaka, H. Kontani, and H. Aoki, Phys. Rev. Lett. **101**, 087004 (2008).
[22] T. Yildirim, Phys. Rev. Lett. **101**, 057010 (2008).
[23] F. Ma and Z.-Y. Lu, Phys. Rev. B **78**, 033111 (2008).
[24] V. Cvetkovic and Z. Tesanovic, arXiv:0804.4678 (unpublished).
[25] J. P. Perdew and Y. Wang, Phys. Rev. B **46**, 12947 (1992).
[26] P. E. Blöchl, Phys. Rev. B **50**, 17953 (1994).
[27] G. Kresse and J. Furthmüller, Phys. Rev. B **54**, 11169 (1996).
[28] S. Kitao, Y. Kobayashi, S. Higashitaniguchi, M. Saito, Y. Kamihara, M. Hirano, T. Mitsui, H. Hosono, and M. Seto, J. Phys. Soc. Jpn. **77**, 103706 (2008).
[29] It is well-known that approximate exchange-correlation functionals, such as PW91, can significantly underestimate the values of energetic characteristics. More reliable values of E_1, E_2, and E_3, as well as those of Fe magnetic moments, could be, in principle, obtained by more accurate quantum-mechanical methods, which include exact exchange interaction and allow for coupling of different many-electron states. However, these methods become prohibitively expensive if the relaxation of a large supercell needs to be considered.
[30] G. A. Gehring and K. A. Gehring, Rep. Prog. Phys. **38**, 1 (1975).
[31] C. de la Cruz, Q. Huang, J. W. Lynn, J. Li, W. Ratcliff II, J. L. Zaretsky, H. A. Mook, G. F. Chen, J. L. Luo, N. L. Wang, and P. Dai, Nature (London) **453**, 899 (2008).
[32] E. Bucher, R. J. Birgeneau, J. P. Maita, G. P. Felcher, and T. O. Brun, Phys. Rev. Lett. **28**, 746 (1972).
[33] E. Pytte and K. W. H. Stevens, Phys. Rev. Lett. **27**, 862 (1971).
[34] C. Detlefs, A. H. M. Z. Islam, T. Gu, A. I. Goldman, C. Stassis, P. C. Canfield, J. P. Hill, and T. Vogt, Phys. Rev. B **56**, 7843 (1997).
[35] $N_{AF2}(\varepsilon)$ in the **T** phase (not shown) and **O** phase differ slightly near ε_F in that $N_{AF2}(\varepsilon_F)$ decreases and $N_{AF2}(\varepsilon)$ elsewhere in the $\sim$0.2 eV vicinity of ε_F increases as a result of the $\mathbf{T} \rightarrow \mathbf{O}$ transition, which can be interpreted as the effect of the cooperative Jahn-Teller distortion. However, this effect is much smaller than the difference between $N_{AF2}(\varepsilon)$ and $N_{AF1}(\varepsilon)$.
[36] T. Y. Chen, Z. Tesanovic, R. H. Liu, X. H. Chen, and C. L. Chien, Nature (London) **453**, 1224 (2008).
[37] A. A. Abrikosov, Physica C **468**, 97 (2008).